The Celestial Reference Frame at X/Ka-band (8.4/32 GHz)

C. S. Jacobs, J. E. Clark, L. J. Skjerve, O. J. Sovers, C. Garcia-Miro, S. Horiuchi

Abstract We have constructed an X/Ka-band (8.4/32 GHz) celestial reference frame using fifty-two 24-hour sessions with the Deep Space Network. We detected 455 sources covering the full 24 hours of right ascension and declinations down to -45 deg. Comparison of 404 X/Ka sources in common with the S/X-band (2.3/8.4 GHz) ICRF2 shows wRMS agreement of 213 micro-arcsec (μas) in $\alpha\cos\delta$ and 282 μas in δ. There is evidence for systematic errors at the 100 μas level. Known errors include limited SNR, lack of phase calibration, troposphere mismodelling, and limited southern geometry. Compared to X-band, Ka-band allows access to more compact source morphology and reduced core shift. Existing X/Ka data and simulated Gaia data predict a frame tie precision of 10–15 μas (1-σ, per 3-D rotation component) with anticipated improvements reducing that to 5–10 μas per component.

Keywords reference systems, celestial frame, ICRF, frame tie, Gaia, catalogs, astrometry, interferometry, VLBI, radio continuum, X/Ka-band, Ka-band, galaxies: active galactic nuclei, quasars, blazars

C.S. Jacobs, J.E. Clark, L.J. Skjerve, and O.J. Sovers
Jet Propulsion Laboratory, California Institute of Technology, 4800 Oak Grove Dr., Pasadena CA 91109.

C.Garcia-Miro
Ingenieria y Servicios Aeroespaciales,
Instituto Nacional de Técnica Aeroespacial/NASA
Madrid Deep Space Communication Complex,
Paseo del Pintor Rosales, 34 bajo, E-28008 Madrid, Spain

S. Horiuchi
C.S.I.R.O. Astronomy and Space Science/NASA,
PO Box 1035, AU Tuggeranong ACT 2901, Australia

1 Introduction

For over three decades now, radio frequency work in global astrometry, geodesy, and deep space navigation has been done at S-band (2.3 GHz) and X-band (8.4 GHz). While this work has been tremendously successful in producing 100 μas level global astrometry (*e.g.* Ma et al, 2009) and sub-cm geodesy, developments made over the last decade have made it possible to consider the merits of moving to a new set of frequencies. In this paper we present global astrometric results from X/Ka (8.4/32 GHz) observations.

Advantages: Moving the observing frequencies up by approximately a factor of four has several advantages. For NASA's Deep Space Network, the driver is the potential for higher data rates for telemetry signals from deep space probes. Other advantages include 1) the spatial distribution of flux becomes significantly more compact (Charlot *et al*, 2010) lending hope that the positions will be more stable over time, 2) Radio Frequency Interference (RFI) at S-band would be avoided, 3) Ionosphere and solar plasma effects on group delay are reduced by a factor of 15!

Disadvantages: While these are very significant advantages, they do not come without a price. The change from 2.3 / 8.4 GHz to 8.4 / 32 GHz moves one closer to the water line at 22 GHz and thus increases the system temperature from a few Kelvins per atmospheric thickness up to 10–15 Kelvins per atmosphere or more. Thus one becomes much more sensitive to weather. Furthermore, the sources themselves are in general weaker and many sources are resolved. Also, with the observing wavelengths shortened by a factor of 4, the coherence times are shortened so that practical integration times are a few minutes or less—even in relatively dry climates. The shorter wavelengths also imply that the

antenna pointing accuracy requirements must be tightened by the same factor of 4. The combined effect of these disadvantages is to lower the system sensitivity. Fortunately, advances in recent years in recording technology make it feasible and affordable to offset these losses in sensitivity by recording more bits. Thus while most of the X/Ka data presented in this paper used the same overall 112 Mbps bit rate as previous S/X work, recent data were taken at 448 Mbps with an increase to 2048 Mbps hoped for within the next year or two.

This paper is organized as follows: We will describe the observations, modelling, and present the results. Next, we will estimate the accuracy by comparing to the S/X-based ICRF2 (Ma et al, 2009) including a look at zonal errors. This will be complemented by a discussion of the error budget and the potential for improving the geometry of our network by adding a southern station. Lastly, we will discuss the potential for linking the X/Ka radio frame and the Gaia optical frame.

2 The VLBI Observations

The results presented here are from fifty-two Very Long Baseline Interferometry (VLBI) observing sessions of $\sim$24 hour duration done from July 2005 until September 2010 using NASA's Deep Space Stations (DSS) 25 or DSS 26 in Goldstone, California to either DSS 34 in Tidbinbilla, Australia or DSS 54 or DSS 55 outside Madrid, Spain to form interferometric baselines of 10,500 and 8,400 km length, respectively. We recorded VLBI data simultaneously at X-band (8.4 GHz) and Ka-band (32 GHz). Initially, sampling of each band was at 56 Mbps while more recent passes used 160/288 Mbps at X/Ka. Each band used a spanned bandwidth of $\sim$360 MHz. The data were filtered, sampled, and recorded to the Mark4 or Mark5A VLBI systems. The data were then correlated with the JPL BlockII correlator (O'Connor, 1987) or the JPL SOFTC software correlator (Lowe, 2005). Fringe fitting was done with the FIT fringe fitting software (Lowe, 1992). The measurements covered the full 24 hours of right ascension and declinations down to -45 deg. Individual observations were about 1 to 2 minutes in duration.

3 Modelling

The above described set of observations were then modelled using the MODEST software (Sovers, Fanselow, & Jacobs, 1998). A priori Earth orientation was fixed to the MHB nutation model (Mathews *et al*, 2002) and the empirically determined UT1-UTC and Polar Motion of the Space 2008 series (Ratcliff & Gross, 2010). The celestial frame was aligned to the ICRF2 defining sources (Ma *et al*, 2009) using a no-net-rotation constraint (Jacobs *et al* 2010). Station velocities were estimated; station locations were estimated with a 1 cm constraint per component to a decades-long S/X-band VLBI solution.

4 Results

In all, we detected 455 extragalactic radio sources which covered the full 24 hours of RA and Declinations down to -45 deg. In Fig. 1 these sources are plotted using Hammer's (1892) equal-area projection to show their locations on the sky. RA$=0$ is at the center. The ecliptic plane is shown by the sinusoidal-shaped curve and the Galactic plane is indicated by the Ω-shaped curve. The source symbols indicate the 1-σ formal declination uncertainties with the value ranges indicated in the figure's legend. Note that the declination precision drops as one moves toward the south. This is a result of having significantly less data on the California to Australia baseline combined with the need to observe sources closer to the horizon as declination moves south, thus incurring greater error from higher system temperatures and tropospheric mis-modelling.

5 Accuracy: X/Ka vs. S/X comparisons

Experience shows that formal uncertainties tend to underestimate true errors. An independent estimate of position errors was obtained by comparing our X/Ka-band positions to the S/X-based ICRF2. For 404 common sources, the weighted RMS (wRMS) differences are 213 μas in $\alpha\cos\delta$ and 282 μas in δ.

6 Zonal Errors

Section 5 gave a measure of overall coordinate agreement. We now turn to X/Ka−S/X differences which are systematically correlated as a function of position on the sky. The slopes of α and δ differences vs. α and δ:

$\Delta\alpha\cos\delta$ vs. $\alpha = 3.5 \pm 1.7$ μas/hr
$\Delta\delta$ vs. $\alpha = 1.8 \pm 1.2$ μas/hr
$\Delta\alpha\cos\delta$ vs. $\delta = 0.4 \pm 0.5$ μas/deg
$\Delta\delta$ vs. $\delta = 1.1 \pm 0.9$ μas/deg

The most significant slope is $\Delta\alpha\cos\delta$ vs. α at 2.1σ. Note that the use of full correlations had a significant effect on the determination of these slopes. Fig. 2 shows in detail the declination differences vs. declination in the sense (X/Ka − S/X).

7 Discussion of Error Budget

Having assessed the size of errors in our positions using the much larger ICRF2 S/X data set as a standard of accuracy, we now discuss the major contributions to the errors in the X/Ka measurements: SNR, instrumentation, and troposphere. The trend of the weighted RMS group delay vs. the Ka-band SNR shows that for SNR $<$ 15 dB, the thermal error dominates the error budget. For higher SNRs, troposphere and instrumentation errors become more important. Binning of wRMS delay vs. airmass thickness shows that troposphere is not the dominant error due to the generally low SNRs just mentioned. However, the phase rates (which carry much less weight in the fit) are dominated by errors from tropospheric mismodelling, thus hinting that troposphere will become more important as our SNR improves with increased data rates. Lastly, we have errors from un-calibrated instrumentation. A proto-type phase calibrator was developed in order to calibrate the signal path from the feed to the sampler (Hammel *et al*, 2003). Test data indicate an approximately diurnal instrumental effect with ∼180 psec (5.4cm) RMS. Although the data themselves can be used to estimate instrumental parameters which partially characterize this effect, operational phase calibrators are being built in order to make direct reliable calibrations of the instrumentation .

8 Southern Geometry Simulation

Besides the three classes of measurement errors described above, our reference frame suffers from a very limited geometry—we have only one station in the southern hemisphere. In order to better understand this limitation, we simulated the effect of adding a second southern station (Bourda, Charlot, & Jacobs, 2010). Data from 50 real X/Ka sessions were augmented by simulated data for 1000 group delays each with SNR = 50 on a ∼9000 km baseline: Australia to S. America or S. Africa. The resulting solution extended Declination coverage to the south polar cap region: −45 to −90 deg. Precision in the south cap region was ∼200 μas (1 nrad) and in the mid south precision was 200–1000 μas, all with just a few days observing. We conclude that adding a second southern station would greatly aid our X/Ka frame's accuracy. In fact, the resulting four station network should compete well in astrometric accuracy with the historical S/X network and its ICRF2.

9 Potential frame tie to Gaia optical frame

The Gaia mission (2012 launch) is expected to measure 10^9 objects with 10s of μas precision including 500,000 quasars of which ∼ 2000 are expected to be both optically bright ($V < 18$) and radio loud (30–300+ mJy).

We have 336 sources with optical counterparts (Veron-Cetty & Veron, 2010) with visual (500–600 nm) magnitude, V, bright enough to be detected by Gaia ($V < 20$ mag). Of these, 130 are bright by Gaia standards ($V < 18$).

Description	Magnitude range	Number	Percent
Bright	$0 < V < 18$	130	29 %
Detectable	$18 < V < 20$	206	45 %
Undetectable	$20 < V$	51	11 %
Unmeasured	V unknown	68	15 %

Table 1 Optical magnitude categories of X/Ka sources

Using existing X/Ka-band position uncertainties and simulated Gaia uncertainties (corrected for ecliptic latitude, but not for V−I color), we did a covariance study which predicts that the 3-D rotation between the X/Ka frame and the Gaia frame could be estimated

with a precision of 10–15 μas per rotation angle (1-σ). The result is dominated by X/Ka uncertainties which have potential for a factor of two or more improvement by the time of the final Gaia catalog in 2021. Thus a frame tie precision of 5–10 μas may be possible.

Angle	Formal Uncertainty
R_x	$\pm$16 μas
R_y	$\pm$13 μas
R_z	$\pm$11 μas

Table 2 Estimated precision of X/Ka to Gaia frame tie

10 Conclusions

A celestial frame at X/Ka-band (8.4/32 GHz) has been constructed with 455 sources. For the 404 sources common to X/Ka and the S/X-based ICRF2, we find positional agreement of 213 μas (1 nrad) in $\alpha\cos\delta$ and 282 μas (1.4 nrad) in δ. Improvements in data rates and instrumental calibration are projected to allow better than 200 μas (1 nrad) accuracy within the next few years. Simulations of adding another southern station predict better than 200 μas accuracy for the southern polar cap within a very short time of adding data from an all southern baseline. This gives hope that better than 100 μas accuracy over the full sky might be achieved within a few years of adding a southern baseline. Lastly, simulations of the X/Ka sources with optical counterparts bright enough to be detectable by the Gaia mission show potential for a frame tie with 5–15 μas precision and reduced systematic errors from source structure and core shift compared to S/X-band.

11 Acknowledgements

This paper is dedicated to our colleague Lyle J. Skjerve who passed on to the next life while this paper was in preparation. He is missed. The research described herein was performed at the Jet Propulsion Laboratory of the California Institute of Technology, under a contract with the National Aeronautics and Space Administration. Government sponsorship acknowledged.

References

Bourda, G., P. Charlot, and C.S. Jacobs, (2010) 'Future Radio Reference Frames and Implications for the Gaia Link,' Proc. of ELSA Conference: Gaia at the Frontiers of Astrometry, Sevres, France.
ftphip.obspm.fr/gaia2010/IMG/pdf/Poster_Bourda.pdf

Charlot, P., D.A. Boboltz, A.L. Fey, E.B. Fomalont, B.J. Geldzahler, D. Gordon, C.S. Jacobs, G.E. Lanyi, C. Ma, C.J. Naudet, J.D. Romney, O.J. Sovers, and L. D. Zhang, (2010), 'The Celestial Reference Frame at 24 and 43 GHz II. Imaging, AJ, 139, 5, 1713. doi: 10.1088/0004-6256/139/5/1713
http://iopscience.iop.org/1538-3881/139/5/1713/

Hamell, R., B. Tucker, & M. Calhoun, (2003), 'Phase Calibration Generator,' NASA JPL IPN Prog. Report, 42-154, pp. 1–14.
tmo.jpl.nasa.gov/progress_report/42-154/154H.pdf

Hammer, E., (1892) 'Über die Planisphäre von Aitow und verwandte Entwürfe, insbesondere neue flächentreue ähnlicher Art,' Petermanns Mitt., 38, pp. 85–87.

Jacobs, C.S., M.B. Heflin, O.J. Sovers, and J.A. Steppe, (2010), 'CRF Rotational Alignment Significantly Altered by RA-Dec Correlations,' IVS 2010 Gen. Meeting Proc., eds. D. Behrend & K. D. Baver, NASA/CP-2010, IVS Analysis Session, Hobart, Tasmania, Australia.
ftp://ivscc.gsfc.nasa.gov/pub/general-meeting/2010/presentations/GM2010_AW_jacobs.pdf

Lowe, S.T., (1992) *Theory of Post-BlockII VLBI Observable Extraction*, JPL Pub. 92-7, Pasadena CA.
ntrs.nasa.gov/archive/nasa/casi.ntrs.nasa.gov/19940009399_1994009399.pdf

Lowe, S. T., (2005) *SOFTC: A Software VLBI Correlator*, JPL section 335 internal document, Pasadena, CA.

Ma, C., *et al.*, (2009), editors: A.L. Fey, D. Gordon & C.S. Jacobs, IERS Tech Note 35: 'The 2nd Realization of the ICRF by VLBI,' IERS, Frankfurt, Germany, Oct. 2009.
http://www.iers.org/nn_11216/IERS/EN/Publications/TechnicalNotes/tn35.html

Mathews, P. M., T. A. Herring, and B. A. Buffet, (2002), 'Modeling of Nutation and Precession: New nutation series for Nonrigid Earth and Insights into the Earth's Interior,' JGR, 107, B4, 10.1029/2001JB000390.
www.agu.org/journals/jb/jb0204/2001JB000390/

O'Connor, T., (1987) *Introduction to the BlockII Correlator hardware*, JPL internal publication, Pasadena CA.

Ratcliff, J.T., and R.S. Gross, (2010), *Combinations of Earth Orientation Measurements: Space 2008, COMB2008, and POLE 2008*, JPL Publication 10-4, Pasadena CA.
http://hdl.handle.net/2014/41512

Sovers, O.J., J.L. Fanselow, & C.S. Jacobs, (1998), 'Astrometry, Geodesy with Radio Interferometry: Expts., Models, Results,' Rev. Mod. Phys., 70, 4, 1393–1454.
link.aps.org/doi/10.1103/RevModPhys.70.1393
doi: 10.1103/RevModPhys.70.1393

Veron-Cetty & Veron, (13th ed.), A&A, 51, Feb. 2010.
vizier.cfa.harvard.edu/viz-bin/VizieR?-source=VII/258

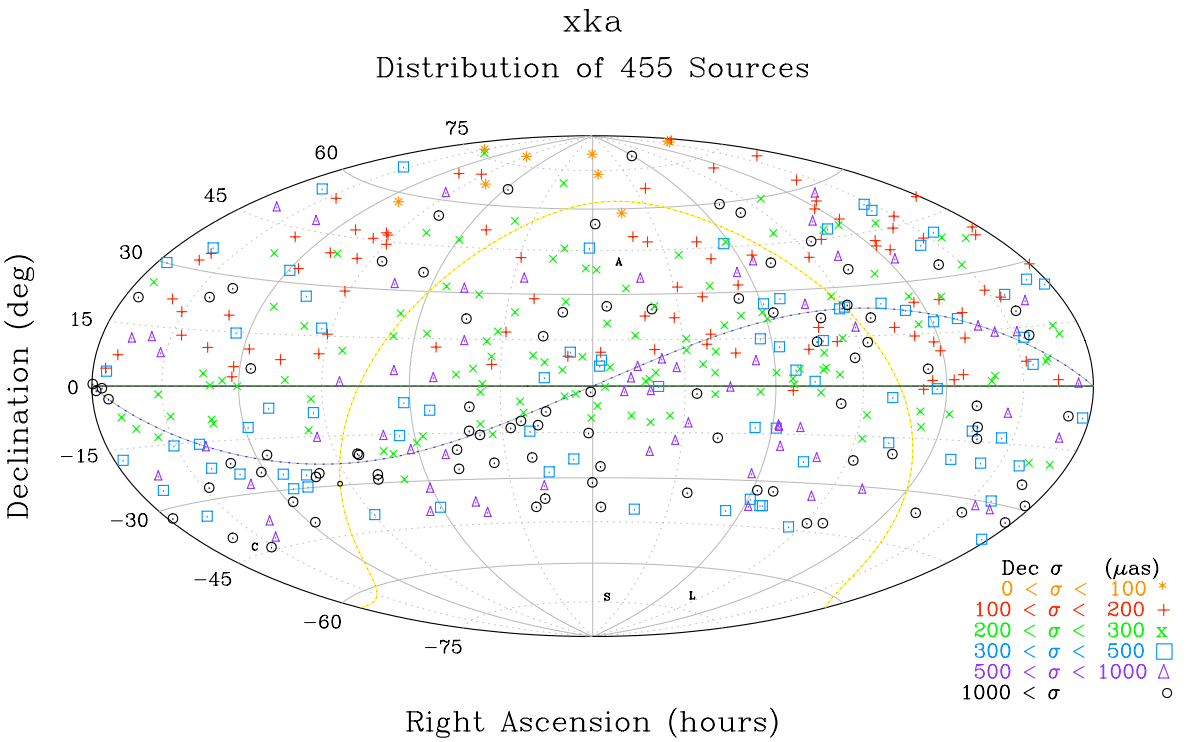

Fig. 1 Distribution of 455 X/Ka-band sources detected to date. Symbols indicate 1-σ formal declination uncertainties as defined in the legend at lower right. $(\alpha, \delta) = (0,0)$ is at the center. The ecliptic plane is indicated by the sinusoidal curve. The galactic plane is indicated by the Ω-shaped curve. Note the trend for decreasing declination precision moving southward. Local galactic neighborhood indicated by A, C, S, L: Andromeda, Centaurus-A, Small & Large Magellanic clouds (none observed at X/Ka).

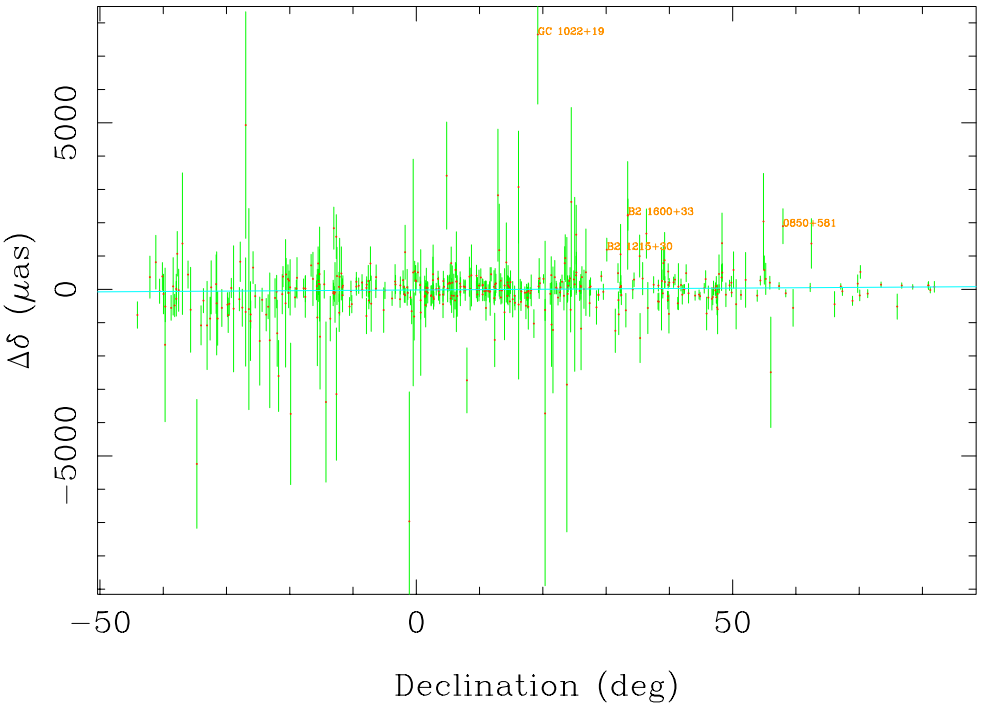

Fig. 2 Declination differences vs. declination for X/Ka − S/X-based ICRF2. The slope is 1.1 ± 0.9 μas/deg.